

WEAK LENSING POWER SPECTRUM RECONSTRUCTION BY COUNTING GALAXIES.– I: THE ABS METHOD

XINJUAN YANG¹, JUN ZHANG², YU YU³, PENGJIE ZHANG^{2,4}

¹ INSTITUTE FOR ADVANCED PHYSICS & MATHEMATICS, ZHEJIANG UNIVERSITY OF TECHNOLOGY, HANGZHOU, 310032, CHINA

² DEPARTMENT OF ASTRONOMY, SHANGHAI JIAO TONG UNIVERSITY, 955 JIANCHUAN ROAD, SHANGHAI, 200240

³ KEY LABORATORY FOR RESEARCH IN GALAXIES AND COSMOLOGY, SHANGHAI ASTRONOMICAL OBSERVATORY, 80 NANDAN ROAD, SHANGHAI, 200030, CHINA

⁴ IFSA COLLABORATIVE INNOVATION CENTER, SHANGHAI JIAO TONG UNIVERSITY, SHANGHAI 200240, CHINA

Draft version October 19, 2018

ABSTRACT

We propose an Analytical method of Blind Separation (ABS) of cosmic magnification from the intrinsic fluctuations of galaxy number density in the observed galaxy number density distribution. The ABS method utilizes the different dependences of the signal (cosmic magnification) and contamination (galaxy intrinsic clustering) on galaxy flux, to separate the two. It works directly on the measured cross galaxy angular power spectra between different flux bins. It determines/reconstructs the lensing power spectrum analytically, without assumptions of galaxy intrinsic clustering and cosmology. It is unbiased in the limit of infinite number of galaxies. In reality the lensing reconstruction accuracy depends on survey configurations, galaxy biases, and other complexities, due to finite number of galaxies and the resulting shot noise fluctuations in the cross galaxy power spectra. We estimate its performance (systematic and statistical errors) in various cases. We find that, stage IV dark energy surveys such as SKA and LSST are capable of reconstructing the lensing power spectrum at $z \simeq 1$ and $\ell \lesssim 5000$ accurately. This lensing reconstruction only requires counting galaxies, and is therefore highly complementary to the cosmic shear measurement by the same surveys.

Keywords: cosmology: observations: large-scale structure of universe: dark matter: dark energy

1. INTRODUCTION

Weak gravitational lensing probes the large scale structure and geometry of the universe (Bartelmann & Schneider 2001; Refregier 2003; Hoekstra & Jain 2008; Munshi et al. 2008). It contains valuable information of fundamental physics, such as dark matter, dark energy and the nature of gravity at cosmological scales (Bartelmann & Schneider 2001; Refregier 2003; Albrecht et al. 2006; Hoekstra & Jain 2008; Munshi et al. 2008; Weinberg et al. 2013). A major goal of precision cosmology is to both measure and model weak lensing accurately.

Despite of being a weak cosmological signal, weak lensing can be measured and has been measured in various ways. (1) The most comprehensively studied method is to measure the lensing distorted galaxy shapes. Existing surveys such as CFHTLenS (Heymans et al. 2012; Kilbinger et al. 2013; Fu et al. 2014), SDSS (Huff et al. 2014) and RCSLenS (Hildebrandt et al. 2016) have already measured this cosmic shear signal robustly. The measurement precision will be further improved by ongoing surveys such as KiDS¹, DES² and HSC³. For example, KiDS has presented intermediate results based on observations of 450 deg² (Hildebrandt et al. 2017). DES has also measured cosmic shear in its science verification data (Chang et al. 2015; Jarvis et al. 2016; Becker et al. 2016). Eventually, the planned wider/deeper stage IV

surveys such as Euclid⁴ and LSST⁵ will achieve 1% or better precision. (2) Weak lensing distorts CMB sky (Seljak 1996), which enables the reconstruction of lensing deflection over the sky (Seljak & Zaldarriaga 1999; Okamoto & Hu 2003). Detection of this CMB lensing effect in the WMAP temperature-galaxy cross correlations was first reported by Smith et al. (2007); Hirata et al. (2008). Cross correlations between lensing B-mode polarization and the large scale structure have been detected recently (SPTpol, Hanson et al. (2013); POLARBEAR, Ade et al. (2014a,b); ACTpol, van Engelen et al. (2015)). The lensing auto power spectrum, which is cosmologically more useful, has been reconstructed by ACT (Das et al. 2011), SPT (van Engelen et al. 2012), POLARBEAR (Ade et al. 2014b), and Planck (Planck Collaboration et al. 2014, 2016). In particular Planck has achieved the most significant detection at a level of 40σ . (3) The lensing induced magnification in galaxy/supernovae flux and size provides an alternative to cosmic shear (e.g. Dodelson & Vallinotto (2006); Cooray et al. (2006); Vallinotto et al. (2011); Heavens et al. (2013); Huff & Graves (2014); Duncan et al. (2014); Alsing et al. (2015); Zhang (2015)). It has enabled recent detections (e.g. Schmidt et al. (2012); Duncan et al. (2016)).

Gravitational lensing not only distorts galaxy images, but also changes the spatial distribution of galaxies (Bartelmann 1995; Bartelmann & Schneider 2001). In

Email me at: zhangpj@sjtu.edu.cn

¹ <http://kids.strw.leidenuniv.nl>

² <https://www.darkenergysurvey.org/>

³ <http://www.naoj.org/Projects/HSC/index.html>

⁴ <http://sci.esa.int/euclid/>

⁵ <http://www.lsst.org/lsst/>

principle, this cosmic magnification (magnification bias) effect can also be used to measure weak lensing. It has several appealing advantages. It is free of point spread function (PSF) and intrinsic alignment that cosmic shear measurement suffers severely (Mandelbaum et al. (2015); Troxel & Ishak (2015) and references therein). It has less stringent requirements on galaxy observation. For example, cosmic shear measurement require galaxies to be sufficiently large and bright. But in principle smaller or fainter galaxies, as long as above the detection limit, can all be used for cosmic magnification measurement (Zhang & Pen 2005, 2006). Therefore for the same survey there will be significantly more galaxies useful for cosmic magnification measurement than for cosmic shear measurement.

Nevertheless, in reality cosmic magnification (magnification bias) is usually overwhelmed by intrinsic fluctuations in galaxy number density. And even worse, such intrinsic galaxy density fluctuations are spatially correlated, even over scales of $\sim 100\text{Mpc}/h$. This galaxy intrinsic clustering is the major obstacle of lensing reconstruction through cosmic magnification. It is analogous to the intrinsic alignment in cosmic shear measurement, but more severe. To avoid this problem, cosmic magnification is usually measured indirectly, through cross correlations between background populations such as quasars and foreground galaxies. It was first detected using SDSS galaxies as foreground population and SDSS quasars as background population (Scranton et al. 2005). It was then detected using various other data sets (Hildebrandt et al. 2009; Ménard et al. 2010; Wang et al. 2011; Morrison et al. 2012; Hildebrandt et al. 2013; Bauer et al. 2014; González-Nuevo et al. 2014; García-Fernandez et al. 2016). It can also be detected in galaxies behind galaxy clusters (e.g. Ford et al. (2014); Chiu et al. (2016)) and in high redshift galaxies (e.g. Wyithe et al. (2011)), where the lensing magnification is stronger.

However, since the above cross correlation measurements are subject to the (foreground) galaxy bias, their cosmological applications are limited. For the purpose of precision cosmology, the measurement of the lensing auto correlation instead of galaxy-galaxy lensing is more desired. To do so, we need to separate the magnification bias from the galaxy intrinsic clustering, both at map level or at the level of two-point correlation of the same redshift bin. Zhang & Pen (2005) first pointed out that this is in principle feasible, since magnification bias and the intrinsic galaxy clustering depend differently on galaxy flux. The intrinsic clustering is proportional to the galaxy bias, in which the dominant part (the deterministic bias) is always positive. In contrast, the magnification bias changes sign from faint end to bright end. Therefore it is possible to separate the two in flux space. Yang & Zhang (2011) implemented this idea with an iterative solver to reconstruct the lensing convergence map from the surface number density distribution of galaxies within a redshift bin. Yang et al. (2015) implemented the same idea, but with the aim of reconstructing the lensing power spectrum, which is the most important lensing statistics. The major finding is a mathematical proof that the lensing power spectrum can be uniquely determined under the condition of deterministic bias. This lensing reconstruction requires no

further assumptions on the galaxy bias.

A long standing unresolved problem in lensing reconstruction through cosmic magnification is the stochasticity in the galaxy intrinsic clustering. Yang & Zhang (2011); Yang et al. (2015) found that it is the most significant limiting factor. One possible solution is to model it and then marginalize it in parameter fitting. However, being connected with the nonlinear structure formation and complicated process of galaxy formation, theoretical understanding of the galaxy stochasticity is highly challenging and uncertain. Ideally we shall reconstruct weak lensing without priors or modelling of galaxy intrinsic clustering, including its stochasticity.

This paper is the first in a series of papers presenting the ABS method to solve this crucial problem. It no longer requires vanishing stochasticity. It works for general case of galaxy intrinsic clustering. **ABS** in this paper stands for **A**nalytical method of **B**lind **S**eparation of cosmic magnification from the galaxy intrinsic clustering. It is blind in that it relies on no assumptions on the galaxy intrinsic clustering. It is analytical in that the lensing power spectrum is determined by an analytical formula that we recently discovered, instead of numerical fittings of many unknown parameters. It is unbiased when the survey is sufficiently powerful that shot noise in the observed galaxy distribution can be well controlled. Here we advertise that the ABS method has other applications. We have demonstrated its power in CMB B-mode foreground removal (Zhang et al. 2016).

This paper is organized as follows. We describe the methodology in §2. We demonstrate that its applicability is within the reach of stage IV dark energy projects such as LSST and SKA (§3). We carry out much more comprehensive tests to further demonstrate its generality in §4. We discuss and summarize in §5. We caution that many tests are against highly hypothetical cases, and are only served for evaluating the generality of the ABS method. In a companion paper we will combine with N-body simulations and galaxy mocks to more reliably quantify its realistic performance for realistic surveys.

2. THE ABS METHOD

In the weak lensing regime, the galaxy number overdensity after lensing is given by (e.g. Bartelmann (1995))

$$\delta_g^L = g\kappa + \delta_g. \quad (1)$$

Here κ is the lensing convergence that we want to measure, and δ_g is the intrinsic galaxy number overdensity that we want to eliminate. The prefactor $g = 2(\alpha - 1)$ is determined by $n(F)$, the average number of galaxies per flux interval. For a narrow flux bin, $\alpha \equiv -d \ln n / d \ln F - 1$.⁶ Cosmic magnification (magnification bias) has a specific flux dependence $g(F)$, which is in general different to the flux dependence of the contamination (δ_g). Therefore in principle the signal and the contaminations can be separated in flux space. This motivates us to split galaxies in a redshift bin into N_F flux/luminosity bins and then carry out weak lensing reconstruction in flux space (Zhang & Pen 2005; Yang & Zhang 2011;

⁶ Notice that this is slightly different to the originally derived expression for the number density fluctuation over a flux threshold (Bartelmann 1995). In that case, $\alpha = -d \ln N / d \ln F$, with $N(F) = \int_F^\infty n(F) dF$ as the number of galaxies brighter than F .

Yang et al. 2015). We denote g_i ($i = 1, \dots, N_F$) as the corresponding g of the i -th flux bin. We work in the Fourier space and focus on the determination of lensing power spectrum $C_\kappa(\ell)$ at multipole ℓ .

2.1. The case of ideal measurement

First we consider ideal measurement, in which measurement errors in galaxy clustering (e.g. shot noise) are negligible. For each multipole ℓ bin, we will have N_F^2 angular power spectra C_{ij}^L between the i -th and j -th flux bins,

$$C_{ij}^L(\ell) = g_i g_j C_\kappa(\ell) + (b_i^D(\ell) g_j + b_j^D(\ell) g_i) C_{m\kappa}(\ell) + C_{ij}^g(\ell). \quad (2)$$

These cross power spectra form a symmetric matrix of order N_F , with $N_F(N_F + 1)/2$ independent components. $C_{ij}^g(\ell)$ is the power spectrum of galaxy intrinsic clustering. $b_i^D(\ell)$ is the deterministic bias of galaxies in the i -th flux bin. Notice that it has the superscript ‘‘D’’ and should not be confused with the linear and quadratic bias $b^{(1,2)}$ introduced later in the paper. We explicitly show the scale (ℓ) dependence of bias and emphasize that we do not make any assumptions on this scale dependence. Since the source distribution of galaxies is not infinitesimally thin, it overlaps with the lens distribution. Therefore the intrinsic number overdensity δ_g of galaxies in the i -th (j -th) flux bin is spatially correlated with the magnification bias of galaxies in the j -th (i -th) flux bin. The stochastic part of δ_g is uncorrelated to the matter overdensity δ_m and is therefore uncorrelated to the lensing convergence κ . Therefore, the cross correlation is proportional to the deterministic galaxy bias $b^D(\ell)$. It is also proportional to the cross power spectrum $C_{m\kappa}$ between the matter distribution and the lensing convergence.

C_κ in the first line of Eq. 2 is the signal that we want to measure/reconstruct, and all terms in the second line are contaminations that we want to eliminate. However, due to an intrinsic degeneracy found in Yang et al. (2015), no unique solution of C_κ exists. Fortunately, Yang et al. (2015) found that Eq. 2 can be rewritten as

$$C_{ij}^L = g_i g_j \tilde{C}_\kappa + \tilde{C}_{ij}^g, \quad (3)$$

with

$$\begin{aligned} \tilde{C}_\kappa &\equiv C_\kappa (1 - r_{m\kappa}^2), \quad r_{m\kappa}^2 \equiv \frac{C_{m\kappa}^2}{C_m C_\kappa}, \\ \tilde{C}_{ij}^g &\equiv C_{ij}^g + \tilde{b}_i \tilde{b}_j - b_i^D b_j^D C_m, \\ \tilde{b}_i &\equiv \sqrt{C_m (b_i^D + g_i \frac{C_{m\kappa}}{C_m})}. \end{aligned} \quad (4)$$

Yang et al. (2015) proved that, under the condition of deterministic bias, the solution to \tilde{C}_κ is unique. In the current paper, we will show that the uniqueness of solution holds even with the existence of stochastic bias. Even better, there exists an analytical solution of \tilde{C}_κ .

The intrinsic clustering matrix C_{ij}^g has order N_F , but its rank M (the number of eigenmodes) depends on the degrees of freedom in the intrinsic clustering. For example, if the intrinsic clustering is fully deterministic, its rank $M = 1$. In reality, galaxy clustering contains

stochasticities, so $M > 1$. Numerical simulations suggest that C_{ij}^g has only limited degrees of freedom. We only need 2 or 3 eigenmodes to describe the matrix C_{ij}^{halo} , the cross power spectra of halos between different halo mass bins (Bonoli & Pen 2009; Hamaus et al. 2010). Namely for halos, $M = 2$ or 3. For galaxies, there is so far no quantitative investigation. However, from the viewpoint of halo model, we expect no fundamental difference between C_{ij}^g and C_{ij}^{halo} . The deterministic bias vector \mathbf{b}^D is a linear combination of eigenvectors of \mathbf{C}^g . Then by linear algebra, the rank of matrix C_{ij}^L is $M + 1$, due to the extra linearly independent vector \mathbf{g} in Eq. 2. To identify all these eigenmodes, we need the number of flux bin $N_F \geq M + 1$.

The mathematical structure of Eq. 3 is identical to Eq. 1 in a recent paper by two of the authors (Zhang et al. 2016). This paper proposes an Analytical method of Blind Separation (ABS) of CMB B-mode from foregrounds. There ABS works on the cross band powers between CMB frequency bands,

$$\mathcal{D}_{ij} = f_i^B f_j^B \mathcal{D}_B + \mathcal{D}_{ij}^{\text{fore}}. \quad (5)$$

It solves for the B-mode band power \mathcal{D}_B , without assumptions on the foreground band power $\mathcal{D}_{ij}^{\text{fore}}$. ABS is made possible by two facts. One is that the CMB has a known blackbody frequency dependence $f_i^B \equiv f^B(\nu_i)$. The other is that in principle we can have more frequency bands than the number of independent foreground components. By the correspondences of

$$(F, C_{ij}^L, g_i, \tilde{C}_\kappa, \tilde{C}_{ij}^g) \longleftrightarrow (\nu, \mathcal{D}_{ij}, f_i^B, \mathcal{D}_B, \mathcal{D}_{ij}^{\text{fore}}), \quad (6)$$

Eq. 3 and Eq. 5 (namely Eq. 1 in Zhang et al. (2016)) are indeed mathematically identical. Furthermore, as f_i^B is observationally known in the case of CMB, g_i is observationally known in the case of cosmic magnification. Therefore, the ABS method applies to both cases. So we will simply re-express the results in Zhang et al. (2016) in the language of weak lensing.

- **The solution to \tilde{C}_κ is unique, as long as $M + 1 \leq N_F$.** Then by studies of halo clustering using numerical simulations, once we choose $N_F \geq 4$, weak lensing power spectrum (\tilde{C}_κ) reconstruction is expected to be unique.
- **There exists the following analytical solution for \tilde{C}_κ ,**

$$\tilde{C}_\kappa = \frac{1}{G^T E^{-1} G} = \left(\sum_{\mu=1}^{M+1} G_\mu^2 \lambda_\mu^{-1} \right)^{-1}. \quad (7)$$

Here, λ_μ ($\mu = 1, \dots, M + 1$) is the eigenvalue of the μ -th eigenvector $\mathbf{E}^{(\mu)}$. $E_{\mu\nu} \equiv \mathbf{E}^{(\mu),T} \cdot \mathbf{C}^L \cdot \mathbf{E}^{(\nu)}$ is the projection of the matrix \mathbf{C}^L onto the $M + 1$ dimension space of eigenvectors. $G_\mu \equiv \mathbf{g} \cdot \mathbf{E}^{(\mu)}$. The last expression requires $\mathbf{E}^{(\mu)} \cdot \mathbf{E}^{(\mu)} = 1$ and we will adopt this normalization throughout the paper.

There is one technical issue on the C_κ - \tilde{C}_κ relation to clarify here. The relative difference between the two is

$r_{m\kappa}^2$, where $r_{m\kappa}$ is the cross correlation coefficient between the distribution of source and the lensing field. Usually $r_{m\kappa}^2 \ll 1$ (Yang et al. 2015). For example, for $1.0 < z < 1.2$, $r_{m\kappa}^2 \lesssim 2 \times 10^{-3}$. Therefore $\tilde{C}_\kappa = C_\kappa$ is an excellent approximation for narrow redshift distribution. However, when the width of redshift distribution increases, $r_{m\kappa}^2$ increases. For example, for $0.8 < z < 1.2$, $r_{m\kappa}^2 \simeq 0.01$ over a wide range of ℓ . In this case, we may no longer take $\tilde{C}_\kappa = C_\kappa$, and have to keep in mind that the reconstructed one is $\tilde{C}_\kappa = C_\kappa(1 - r_{m\kappa}^2)$. Fortunately, this does not introduce any new uncertainty in cosmological constraints. The reason is that $r_{m\kappa}$ does not depend on the galaxy bias and can be calculated without introducing extra uncertainties than in C_κ calculation. This means that \tilde{C}_κ is essentially identical to C_κ in cosmological applications.

2.2. Including measurement errors

In reality, the measured (lensed) galaxy clustering is contaminated by shot noise, due to finite number of galaxies. The ensemble average of the shot noise power spectrum can be predicted and subtracted from the observation. What left is

$$C_{ij}^{\text{obs}} = C_{ij}^L + \delta C_{ij}^{\text{shot}}. \quad (8)$$

$\delta C_{ij}^{\text{shot}}$ is the residual shot noise due to statistical fluctuations. It has the following properties,

$$\begin{aligned} \langle \delta C_{ij}^{\text{shot}} \rangle &= 0, \\ \langle \delta C_{ij}^{\text{shot}} \delta C_{km}^{\text{shot}} \rangle &= \frac{1}{2} \sigma_i \sigma_j (\delta_{ik} \delta_{jm} + \delta_{im} \delta_{jk}). \end{aligned} \quad (9)$$

Here, $\sigma_i = (4\pi f_{\text{sky}}/N_i) \times \sqrt{2/[(2\ell+1)\Delta\ell f_{\text{sky}}]}$ is the statistical error caused by shot noise in the band power in the multipole range of $\ell - \Delta\ell/2$ and $\ell + \Delta\ell/2$. f_{sky} is the fractional sky coverage and N_i is the total number of galaxies in the i -th flux bin. Hereafter we will choose the flux bin sizes such that $N_1 = N_2 = \dots = N_{N_F} = N_{\text{tot}}/N_F$, where N_{tot} is the total number of galaxies in all flux bins. We then have $\sigma_1 = \sigma_2 = \dots$, which we denote as σ_{shot} .

$$\sigma_{\text{shot}} = \left(\frac{4\pi f_{\text{sky}}}{N_{\text{tot}}/N_F} \right) \times \sqrt{\frac{2}{(2\ell+1)\Delta\ell f_{\text{sky}}}}. \quad (10)$$

With the presence of shot noise, the rank of matrix C_{ij}^{obs} will be equal to its order N_F . Surprisingly, Eq. 7 can still be implemented in the data analysis, as shown for the case of CMB B-mode (Zhang et al. 2016). Only one straightforward modification is needed to account for shot noise.

- **Step 1.** We compute all N_F eigenmodes of C_{ij}^{obs} .
- **Step 2.** We measure \tilde{C}_κ from Eq. 7, *but only using eigenmodes with $\lambda_\mu > \lambda_{\text{cut}}$.*

Here, λ_{cut} is a cut adopted to filter away unphysical eigenmodes caused by statistical fluctuations of shot noise. Residual shot noise (and other measurement statistical error in general) not only affects the determination of physical eigenmodes, but also induces unphysical eigenmodes with eigenvalues of typical amplitude σ_{shot} .

This roughly sets the value of $\lambda_{\text{cut}} \sim \sigma_{\text{shot}}$. Nevertheless, the above recipe may still miss physical eigenmodes, or fail to exclude unphysical eigenmodes. The impacts will be better understood in the language of λ_μ - c_μ diagnostic of §2.3. The resulting systematic error will be quantified numerically through our simulated data (§3 & 4). The ambiguity in the choice of λ_{cut} will be discussed in §3.4.

The above method of measuring \tilde{C}_κ , even including the determination of M , is completely fixed by the data, and relies on no priors of galaxy intrinsic clustering. Furthermore, it has a precious property that it is unbiased, in the limit of low measurement errors.

2.3. The λ_μ - c_μ diagnostic

The ABS method automatically utilizes the unique (and known) flux dependence of the lensing signal to blindly separate it from overwhelming contaminations of galaxy intrinsic clustering. According to Eq. 7, different eigenmode of the matrix C_{ij}^L has different contribution to the lensing reconstruction. The contribution of the μ -th physical eigenmode is

$$c_\mu \equiv \frac{G_\mu^2/\lambda_\mu}{\sum_{\alpha=1}^{M+1} G_\alpha^2/\lambda_\alpha}. \quad (11)$$

The value of λ_μ determines whether a survey can detect this eigenmode, and the value of c_μ determines whether this eigenmode is relevant for the lensing reconstruction. Statistical error (shot noise as we consider here) in C_{ij}^{obs} may prohibit identification of physical eigenmode, and generate unphysical eigenmodes. The former leads to overestimation of \tilde{C}_κ , while the later leads to underestimation. This λ_μ - c_μ diagnostic is developed in Zhang et al. (2016).

When the measurement error (σ_{shot}) is small, all physical eigenmodes can be identified. But there exists the possibility of unphysical eigenmodes with eigenvalues exceeding λ_{cut} . When a unphysical eigenmode is wrongly included, it results in underestimation by a factor $-c_\mu/(1+c_\mu)$.

In contrast, when σ_{shot} is large and we may fail to detect some physical eigenmodes with small eigenvalues. Missing the μ -th component causes overestimation by a factor of $c_\mu/(1-c_\mu)$. In reality, only those eigenmodes with significant c_μ (e.g. $c_\mu > 0.01$) are relevant for lensing determination. In another word, to achieve 1% level accuracy in the reconstruction, all eigenmodes with $c_\mu > 0.01$ have to be detected. If one of these eigenmodes has $\lambda < \lambda_{\text{cut}} \sim \sigma_{\text{shot}}$, it will be missed in the reconstruction, resulting in significant bias in the reconstructed \tilde{C}_κ .

2.4. Statistical error

Following similar derivation in Zhang et al. (2016) and in the limit of small shot noise fluctuations, we derive the r.m.s. error induced by shot noise,

$$\begin{aligned} \sigma_{C_\kappa} &\equiv \langle \delta \tilde{C}_\kappa^2 \rangle^{1/2} = \eta \times \sigma_{\text{shot}}, \\ \eta &\equiv \left(\sum_{\mu=1}^{M+1} \frac{G_\mu^2}{\lambda_\mu^2} \times \tilde{C}_\kappa^2 \right). \end{aligned} \quad (12)$$

As expected, the statistical error $\sigma_{C_\kappa} \propto \sigma_{\text{shot}}$. The prefactor η is dimensionless, determined by the interplay be

tween the cosmic magnification and the intrinsic clustering, implicitly through λ_μ and $G_\mu \equiv \mathbf{g} \cdot \mathbf{E}^{(\mu)}$. Eq. 12 quantifies the possibility of measuring the lensing power spectrum in the given sky coverage and source redshift, by counting galaxies.⁷

One immediate conclusion from Eq. 7 & 12 is that eigenvectors orthogonal to \mathbf{g} not only have no contribution to the weak lensing reconstruction, but also have no impact on the statistical error of reconstruction. The best case that we can expect for the lensing reconstruction is that all other eigenvectors are orthogonal to \mathbf{g} . In this case, one eigenvector is $\hat{g} \equiv \mathbf{g}/g$, where $g \equiv \sqrt{\sum_i g_i^2}$. The corresponding eigenvalue is $\sum_i g_i^2 \tilde{C}_\kappa$. All other eigenmodes have $G = 0$. We then have $\eta = 1/g^2$. This sets up the lower limit of statistical error of the weak lensing reconstruction, σ_{shot}/g^2 . In general there will be other eigenvectors unorthogonal to \mathbf{g} , so the actual statistical error is larger than the above value.

3. TESTING THE ABS METHOD AGAINST THE FIDUCIAL CASE

The ABS method is unbiased in reconstructing the lensing power spectrum, under the condition of vanishing measurement error in the observed galaxy clustering (e.g. shot noise). In reality, this condition is violated due to limited number of galaxies (and possibly other observation complexities). This causes the realistic performance of the ABS method to depend on many factors, such as survey specifications which determine σ_{shot} , galaxy biases, redshift range, the number of flux bins and cosmology.

We expect σ_{shot} and the galaxy biases as the most important factors affecting the ABS performance. Therefore, for brevity we will fix the cosmology, the number of flux bins, and the redshift range throughout the paper. (1) We adopt a flat Λ CDM cosmology with $\Omega_m = 0.26$, $\Omega_\Lambda = 1 - \Omega_m$, $\Omega_b = 0.044$, $h = 0.72$, $n_s = 0.96$ and $\sigma_8 = 0.8$. The weak lensing angular (2D) power spectrum is calculated by the Limber integral, in which the 3D nonlinear matter power spectrum is calculated using the halofit fitting formula (Smith et al. 2003). (2) We fix the redshift bin $0.8 < z < 1.2$. This is the source redshift range accessible by many cosmic shear surveys such as DES, HSC and LSST. It is therefore convenient for comparison between cosmic shear and cosmic magnification. (3) We fix the number of flux bins as $N_F = 5$. This is implied (but not fixed) by the following considerations. First, the ABS method requires $N_F \geq M + 1$. For most cases that we test, $M = 2$. Therefore $N_F = 3$ is the minimal requirement. Second, we prefer a larger N_F (finer flux bin size) to better capture the different flux dependences of cosmic magnification and galaxy bias. However, N_F can not be arbitrarily large because of increasing shot noise per flux bin with increasing N_F . We then take $N_F = 5$ as our first try. A remaining question of importance is the optimal choice of N_F . In future we will test the ABS method using mocks generated from N-body simulations. At that stage, we will carry out more

⁷ Eq. 12 does not include cosmic variance of the lensing field. This source of statistical error is needed and only needed when we compare the measured lensing power spectrum with the theoretically predicted ensemble average to obtain cosmological parameter constraints.

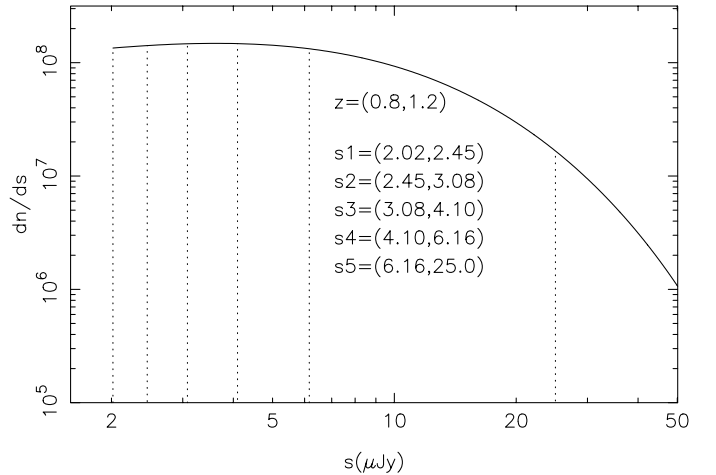


Figure 1. The fiducial number distribution of galaxies (solid line) at $0.8 < z < 1.2$ as a function of 21cm flux s (μJy) in the fiducial SKA-like survey. The vertical dot lines show the ranges of the adopted 5 flux bins. More explanations are provided in §3.1. We caution that this fiducial distribution function is only for the purpose of testing our method, and the actual distribution of galaxies in surveys such as SKA and LSST can be significantly different.

thorough tests of the ABS method against other redshift range, other cosmology, and figure out the optimal choice of N_F .

In this section we test the ABS method against the fiducial case which may resemble what we expect for a stage IV dark energy project. Testing against more general cases will be carried out in the next section.

3.1. The fiducial case

Following our previous papers (Yang & Zhang 2011; Yang et al. 2015), the fiducial survey has $N_{\text{tot}} = 10^9$ galaxies with spectroscopic redshifts determined by 21cm emission line, at $0.8 < z < 1.2$ and over 10^4 deg^2 . Each of these flux bins has $N_{\text{tot}}/N_F = 2 \times 10^8$ galaxies. The galaxy luminosity function, along with the range of flux bins, are shown in Fig. 1. The fiducial sky coverage is $f_{\text{sky}} = 10^4 / (4\pi / (\pi/180)^2)$. As shown in Yang & Zhang (2011), this can be achieved by a SKA like radio array of total collecting area of 1 km^2 , through 21cm observation of neutral hydrogen in galaxies. This requires the full size phase-2 SKA with configuration optimized for a dedicated 5 year 21cm survey. Although this is not likely happening for SKA, it demonstrates that such requirement on galaxy surveys is indeed within the capability of future surveys. Therefore it serves as a suitable example for the purpose of this paper. Furthermore, imaging surveys such as LSST will have billions of galaxies with good photometric redshift measurements, and will be comparable to the fiducial survey in lensing reconstruction through cosmic magnification.

For each fixed ℓ , the intrinsic galaxy power spectra C_{ij}^g ($i, j = 1, \dots, N_F$) is a real, positive definite, and symmetric matrix. According to the spectral decomposition theorem, it can always be decomposed into

$$C_{ij}^g = \sum_{\alpha=1}^M C_\alpha V_i^{(\alpha)} V_j^{(\alpha)}. \quad (13)$$

Here, $\mathbf{V}^{(\alpha)}$ is the α -th eigenvector of the matrix \mathbf{C}^g . C_α is the corresponding eigenvalue, which is real and posi-

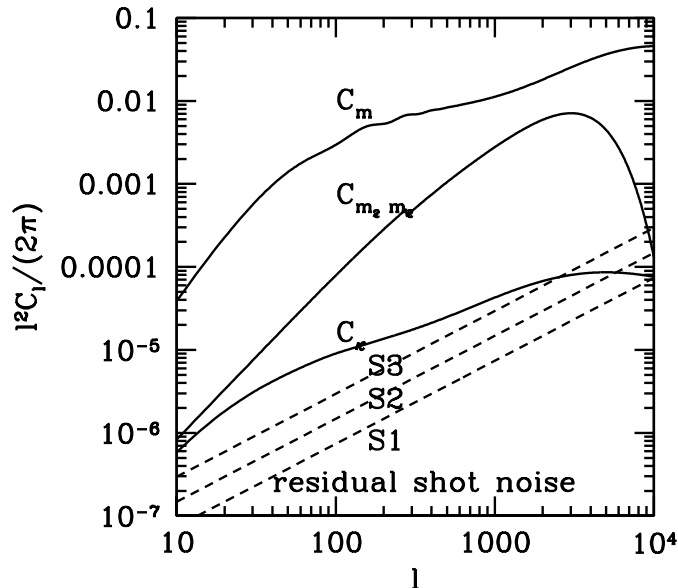


Figure 2. Contaminations of lensing measurement by cosmic magnification (magnification bias), at source redshift $0.8 < z < 1.2$. The measured galaxy clustering power spectrum is the sum of the lensing signal ($\sim C_\kappa$) and the galaxy intrinsic clustering ($\sim C_m, C_{m_2 m_2}$), with measurement error caused by shot noise (dash lines, with bin size $\Delta\ell = 0.4\ell$). The bottom dash line with label “S1” is that of the fiducial survey, and the other two lines with label “S2” and “S4” have a factor of 2 and 4 larger error, respectively.

tive. Bonoli & Pen (2009); Hamaus et al. (2010) found that there are two to three eigenmodes in C_{ij}^g . This motivates us to adopt the following fiducial model of the intrinsic galaxy clustering,

$$C_{ij}^g = b_i^{(1)} b_j^{(1)} C_m + b_i^{(2)} b_j^{(2)} C_{m_2 m_2}. \quad (14)$$

Details of the two biases ($b^{(1,2)}$) and caveats of the model are given in the appendix A. Although not exact, throughout the paper we call $b^{(1)}$ as the linear bias and $b^{(2)}$ as the quadratic bias for convenience. Furthermore, we will approximate $b^{(1)}$ as the deterministic bias shown in Eq. 2. C_m is the angular power spectrum of the projected matter density field. $C_{m_2 m_2}$ is the power spectrum of projected $\delta_{m,R}^2$, where $\delta_{m,R}$ is the matter density smoothed over a radius $R = 1\text{Mpc}/h$.

Fig. 2 shows C_m , $C_{m_2 m_2}$ and C_κ for galaxies at $0.8 < z < 1.2$. As expected, the lensing signal C_κ is a factor of 10^2 to 10^3 smaller than the galaxy intrinsic clustering. The dominant contribution of galaxy intrinsic clustering comes from $b^{(1)}$. But the contribution from $b^{(2)}$ is also significantly larger than the lensing signal. Fig. 2 also shows σ_{shot} , the r.m.s of the residual shot noise of the fiducial survey (the bottom dash line labelled with “S1”). It is significantly smaller than the lensing signal C_κ that we aim to reconstruct in the range $\ell \lesssim 5000$. Later in §3.2 we find that this leads to excellent reconstruction of C_κ at $\ell \lesssim 5000$. The dash line with label “S2” has σ_{shot} enlarged by a factor of 2 and the one with label “S3” enlarged by a factor of 4. The ABS performance against these σ_{shot} will be carried out in §4.

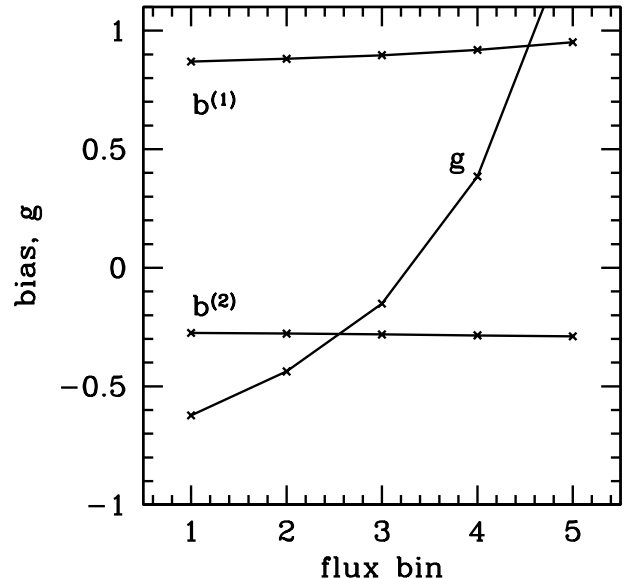


Figure 3. The fiducial galaxy biases and g in the 5 flux bins. $b^{(1)}$ is the linear bias and $b^{(2)}$ is the quadratic bias. The prefactor g in the magnification bias changes sign from faint end to bright end.

The necessary condition to extract the lensing signal (cosmic magnification) from galaxy intrinsic clustering is that the flux dependence of the lensing signal differs from that of the galaxy intrinsic clustering. Namely, in the N_F dimension flux space, the vector \mathbf{g} must not be parallel to the vectors $\mathbf{b}^{1,2}$. Fig. 3 shows the results of $b_i^{(1,2)}$, and g_i ($i = 1, \dots, N_F$). Clearly, the flux dependence of g is significantly different to that of biases. It not only has a stronger dependence, but also changes sign, from negative at faint end to positive at bright end. Unless by coincidence, we expect no eigenvector $\mathbf{v}^{(\alpha)}$ in Eq. 13 to $\propto \mathbf{g}$. Therefore we believe that unbiased lensing reconstruction through cosmic magnification is always doable (Eq. 7), as long as the galaxy survey is sufficiently powerful such that statistical error in the galaxy power spectra measurement is sufficiently small.

3.2. Test results

We assume Gaussian shot noise error $\delta C_{ij}^{\text{shot}}$, with r.m.s. dispersion given by as Eq. 10. We choose a relatively large bin size $\Delta\ell = 0.4\ell$, to suppress shot noise. For each $\delta C_{ij}^{\text{shot}}$, we generate 1000 realizations for the tests. Such realizations are then added to C^L of Eq. 2 to generated 1000 realizations of simulated C_{ij}^{obs} using Eq. 8. We then use the ABS method to process the simulated C_{ij}^{obs} and output \tilde{C}_κ .

The test result is shown in Fig. 4. The thick solid line is the input \tilde{C}_κ .⁸ The thin solid line with label “S1” is the output by our ABS method applied to the fiducial survey. It shows that, our ABS method successfully recovers

⁸ Notice again that for $0.8 < z < 1.2$, $\tau_{m\kappa}^2 \simeq 0.01$, so \tilde{C}_κ is 1% smaller than C_κ . Although the difference is small, it is often comparable to the systematic error of weak lensing reconstruction. Therefore we have to keep it in mind when testing our method.

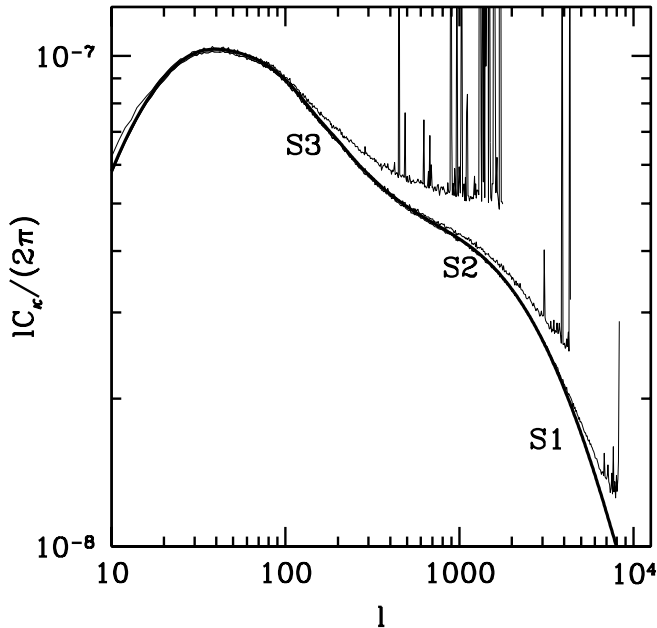


Figure 4. The accuracy of lensing power spectrum reconstruction, for the three cases of residual shot noise in Fig. 2. The thick solid line is the input \tilde{C}_κ and the thin lines are the output by our ABS method, averaged over 1000 realizations of residual shot noise. The reconstruction fails when the residual shot noise is comparable to the lensing signal ($\sigma_{\text{shot}} \sim C_\kappa$), with more exact dependence given by the λ_μ - c_μ plot in Fig. 6.

the input \tilde{C}_κ up to $\ell \sim 5000$. Towards smaller scale, it begins to overestimate the lensing power spectrum and the performance quickly degrades. It eventually becomes unstable at $\ell \gtrsim 7000$. This is caused by the increasing fluctuations of residual shot noise with respect to the lensing signal (Fig. 2). Fig. 4 also shows the test results against the cases of “S2” and “S3” with a factor of 2 and 4 larger σ_{shot} . Clearly the reconstruction is highly sensitive to σ_{shot} . We postpone detailed discussion on such dependence until in §4.

To highlight the reconstruction accuracy, we plot the fractional statistical and systematic error (solid lines) in Fig. 5. Both errors are evaluated averaging over 1000 realizations of residual shot noise. At $\ell \lesssim 1000$, the systematic error is negative, with a relative amplitude of $\sim 1\%$. However at $\ell \gtrsim 2000$, it becomes positive and reaches $\sim 10\%$ at $\ell = 5000$. To understand such behavior of the systematic error, we will resort to the λ_μ - c_μ diagnostic in §3.3. Nevertheless, at $\ell \lesssim 7000$, the systematic error is smaller than the statistical error. Namely, despite the existence of systematic errors, the lensing reconstruction is *statistically unbiased*.

3.3. The λ_μ - c_μ diagnostic for the fiducial case

The fiducial case has three physical eigenmodes, since there are three independent vectors in the N_F dimension flux space ($\mathbf{b}^{(1,2)}$ and \mathbf{g}). The eigenmodes depend on the multipole ℓ . Since the lensing power spectrum suffers from non-negligible uncertainties of baryon physics at $\ell \gtrsim 2000$ (White 2004; Zhan & Knox 2004; Jing et al. 2006; Rudd et al. 2008), $\ell \lesssim 2000$ is most useful for weak lensing cosmology. Therefore we show the result of $\ell = 2000$ (filled circles) in Fig. 6. Since g is negative

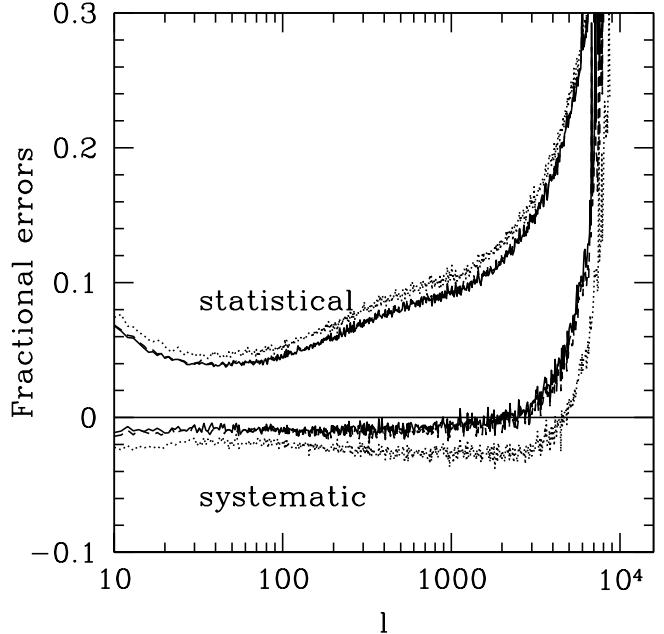


Figure 5. The dependence of lensing power spectrum determination on the cut of eigenvalue λ_{cut} . To highlight the dependences, we show both the relative statistical error and relative systematic error for $\lambda_{\text{cut}} = \sigma_{\text{shot}}$ (solid lines), $\sigma_{\text{shot}}/N_F^{1/2}$ (dot lines) and $2\sigma_{\text{shot}}/N_F^{1/2}$ (dash lines, almost overlap with solid lines). Both statistical and systematic error are estimated from 1000 realizations of simulated data.

at faint end and positive at bright end, $\sum g_i \sim 0$. Since both $b^{(1)}$ and $b^{(2)}$ vary slowly with flux, the two vectors $\mathbf{b}^{(1,2)}$ are nearly orthogonal to \mathbf{g} ($\mathbf{b}^{(1,2)} \cdot \mathbf{g} \sim 0$). Therefore one eigenvector (the second one) is almost perfectly parallel to \mathbf{g} , with c very close to unity. The majority of the intrinsic clustering is absorbed in the first (the largest) eigenmode. Its eigenvalue is $\sim \sum_i C_{ii}^g$, more than two orders of magnitude larger than the second eigenvalue. The ABS method automatically suppresses this eigenmode in the lensing reconstruction, through a small $G_1 \ll 1$ and through $\lambda_1 \gg C_\kappa$. For these reasons, its contribution (c_1) is less than 0.01%. The rest of the intrinsic clustering and the lensing signal enter the third eigenmode. Its eigenvalue is too tiny to be detected in realistic surveys. But since it is almost completely orthogonal to \mathbf{g} ($G_3 \simeq 0$), its contribution is also negligible.

Therefore, there is only one eigenmode (the second eigenmode) relevant to the lensing reconstruction. The corresponding eigenvalue is $\sim \sum_i^{N_F} g_i^2 C_\kappa \sim C_\kappa$. In this case, the condition for accurate lensing reconstruction is $\sigma_{\text{shot}} \ll C_\kappa$. Fig. 2 shows that this condition is well satisfied at $\ell \leq 1000$ and roughly satisfied at $\ell \lesssim 5000$. Therefore our ABS method accurately recovers the input lensing signal. At $\ell \gtrsim 5000$, this condition is no longer satisfied, the second physical eigenmode is not robustly detected, and the reconstruction suffers from non-negligible systematic bias. At $\ell \gtrsim 10^4$, the second physical eigenmode is overwhelmed by residual shot noise. The reconstruction is highly unstable and no longer reliable.

Fig. 6 also shows λ_μ - c_μ for three other cases, corresponding to different biases and different clustering com-

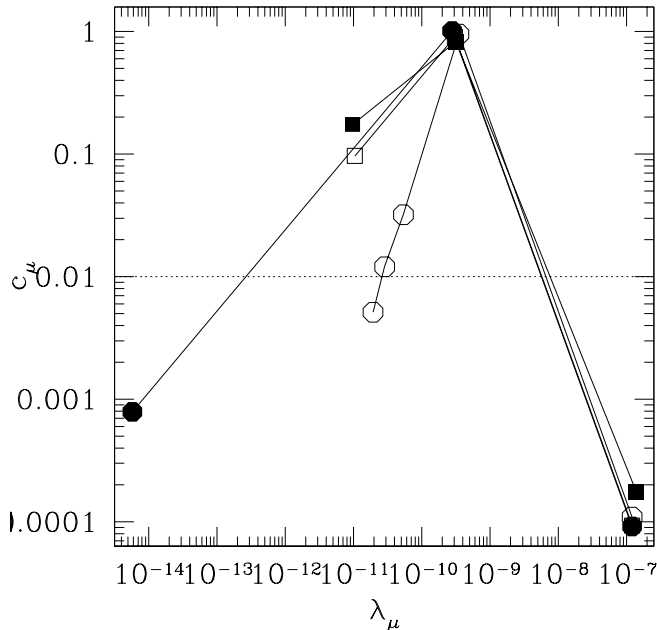


Figure 6. The λ_μ - c_μ plot at $\ell = 2000$. c_μ is the contribution of the μ -th physical eigenmode to the lensing power spectrum reconstruction. We show four cases, the fiducial case (filled circle), shape of $\mathbf{b}^{(1,2)}$ changing by 30% (filled square and open square respectively) described in §4.2.2, and a more complicated case (open circle) described in §4.3. For the reconstruction to be accurate, all physical eigenmodes with significant c_μ must be robustly identified ($\lambda_\mu \gg \sigma_{\text{shot}}$).

ponents. The distribution of λ_μ - c_μ varies significantly among these cases. Later in §3 we will discuss their impacts on the lensing reconstruction.

3.4. The choice of λ_{cut}

The above λ_μ - c_μ diagnostic also tells us that the choice of λ_{cut} is important. λ_{cut} has two-fold and competing impacts on the reconstruction. On one hand, it serves to exclude unphysical eigenmodes caused by statistical measurement errors (residual shot noise in this paper). If it fails and one unphysical eigenmode is wrongly included, the reconstructed \tilde{C}_κ will be underestimated. For this purpose, the larger λ_{cut} , the better. On other hand, the cut may also wrongly exclude physical eigenmodes and cause overestimation of \tilde{C}_κ . To alleviate this problem, the smaller λ_{cut} the better. We try a few choices of λ_{cut} to demonstrate its impact.

Since we know that λ_{cut} should be comparable to σ_{shot} , we try three possibilities, $\lambda_{\text{cut}} = \sigma_{\text{shot}}$, $\sigma_{\text{shot}}/\sqrt{N_F}$, $2\sigma_{\text{shot}}/\sqrt{N_F}$. The results for $\lambda_{\text{cut}} = \sigma_{\text{shot}}$ and $2\sigma_{\text{shot}}/\sqrt{N_F}$ are almost identical (Fig. 5). The smallest cut ($\lambda_{\text{cut}} = \sigma_{\text{shot}}/\sqrt{N_F}$) is more efficient to include physical eigenmodes in the summation of Eq. 7 and thus reduces/improves the overestimation at $\ell \gtrsim 5000$. The price to pay is the higher probability of wrongly including unphysical eigenmodes, and thus stronger/worse underestimation at $\ell \lesssim 2000$. If we focus on the measurement at $\ell < 2000$ of greater cosmological importance, the choice of $\lambda_{\text{cut}} = 2\sigma_{\text{shot}}/\sqrt{N_F}$ or σ_{shot} are both reasonable. Hereafter we will adopt $\lambda_{\text{cut}} = 2\sigma_{\text{shot}}/\sqrt{N_F}$, since it takes the dependence of noise eigenvalue on the num-

ber of flux bins into account.

A remaining task is to fix the optimal λ_{cut} minimizing the systematic error of \tilde{C}_κ determination. A related question is that whether we shall go beyond the step function. For example, given the noise properties (Eq. 9), one can estimate the probability of a given eigenvalue to be contaminated by measurement noise. This may allow the design of an optimal weighting function of λ , instead of a step function used in this paper. This is an important issue for further investigation.

4. TESTING AGAINST MORE GENERAL CASES

The excellent performance of our ABS method to reconstruct the lensing power spectrum for the fiducial case is exciting. It demonstrates its great potential for stage IV dark energy surveys such as LSST and SKA. However, the performance of this method may depend on many factors, for which the fiducial case may no longer be representative. These factors include (1) survey specifications which determine σ_{shot} , (2) galaxy biases and (3) systematic errors in the measured galaxy power spectra. In future we aim to fix these uncertainties by targeting at a specific survey. By targeting at a specific survey and calibrating against N-body simulations, we may fix these factors and make more specific forecast. We will carry out this exercise in a companion paper.

Instead of being specific, here in this methodological paper we will take an alternative approach. We explore a wide range of possibilities, by varying σ_{shot} that a survey can achieve, the amplitude/shape of biases, and extra bias components/systematic errors in the galaxy power spectrum measurement. Since there are so many dimensions of possibilities, we can not fully probe the parameter space. Instead, each time we just vary one configuration and fix the rest as the fiducial ones. These tests demonstrate the generality of the ABS method.

4.1. The impact of survey specifications

The most important factor determining the accuracy of weak lensing reconstruction is the measurement error in the galaxy power spectra. In particular, shot noise fluctuations can bias the lensing reconstruction, as discussed in detail by the λ_μ - c_μ diagnostic.

Fig. 4 shows that the lensing reconstruction strongly depends on σ_{shot} . For the fiducial one, we are able to reconstruct the lensing power spectrum accurately up to $\ell \sim 5000$. But a factor of 2 increase in σ_{shot} renders the accurate measurement at $\ell \gtrsim 2000$ impossible. A further factor of 2 increase renders the accurate measurement at $\ell \gtrsim 300$ impossible. This strong dependence on σ_{shot} comes from the fact that we need the condition $g^2 C_\kappa \gg \sigma_{\text{shot}}$ so that the lensing eigenmode can be robustly identified. From Fig. 3, $g^2 \equiv \sum_i g_i^2 = 2.7$. Let us focus on $\ell = 1000$, where $C_\kappa \simeq 5\sigma_{\text{shot, fid}}$. Therefore, the above condition is well satisfied by the fiducial case (“S1”) and the lensing reconstruction at $\ell = 1000$ is accurate. But it is not satisfied by “S3”, resulting in failure of lensing reconstruction. The case of “S2” falls somewhere between the two.

σ_{shot} is set by survey specifications such as the total number of galaxies N_{tot} and the sky coverage f_{sky} . Since $\sigma_{\text{shot}} \propto f_{\text{sky}}^{1/2}/N_{\text{tot}} \propto \bar{n}^{-1} f_{\text{sky}}^{-1/2}$, successful reconstruction requires sufficiently high galaxy number density \bar{n} and

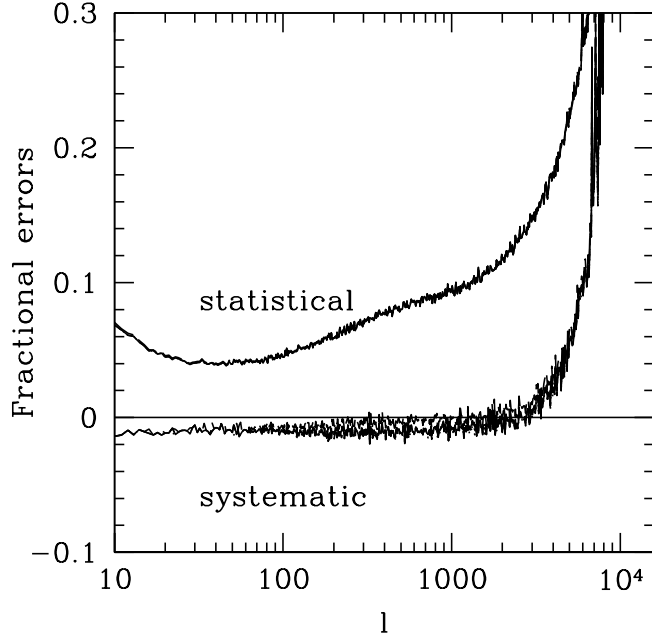


Figure 7. The dependence of lensing power spectrum determination on the amplitude of the linear bias $\mathbf{b}^{(1)}$. We arbitrarily increase the amplitude of $\mathbf{b}^{(1)}$ by a factor of 2 and 4. Neither the statistical nor the systematic error change visibly. However, if we reduce $\mathbf{b}^{(1)}$ by a factor of 10 (dash lines), the systematic error has a small but visible change.

sufficiently large f_{sky} . The fiducial value of σ_{shot} adopted is achieved for a survey with high galaxy number density ($\bar{n} = 28$ galaxies per arcmin² at $0.8 < z < 1.2$), and large sky coverage ($f_{\text{sky}} = 0.24$). The survey requirements are stringent, but within the capability of SKA (Yang & Zhang 2011; Yang et al. 2015).

These requirements may also be satisfied by other surveys. (1) SKA has a proposal to survey 30000 deg² for the detection of 9×10^8 HI galaxies.⁹ However, these are galaxies above 10σ detection threshold. For cosmic magnification measurement, we can use fainter galaxies (e.g. at 5σ), and there are many more of them. Furthermore, for fixing total survey time, smaller sky coverage results in higher galaxy number density. So there is room to improve the cosmic magnification measurement by adjusting the SKA survey strategy. (2) Imaging surveys with reasonably good photo- z can also be used for lensing reconstruction through cosmic magnification. Since we do not need to measure galaxy shapes, we do not require galaxies to be as bright and large as in cosmic shear measurement. Therefore for the same imaging survey, there will be significantly more galaxies useful for lensing magnification measurement than for shear measurement. One possibility is LSST. LSST will have ~ 30 galaxies per arcmin² for cosmic shear measurement. Therefore it will have many more galaxies for the cosmic magnification measurement. One open question is the extra error induced by photo- z errors, which affect both the signal through the determination of g , and the intrinsic clustering. This is to be studied in detail against N-body mocks in the future. (3) Furthermore, we may even choose wider

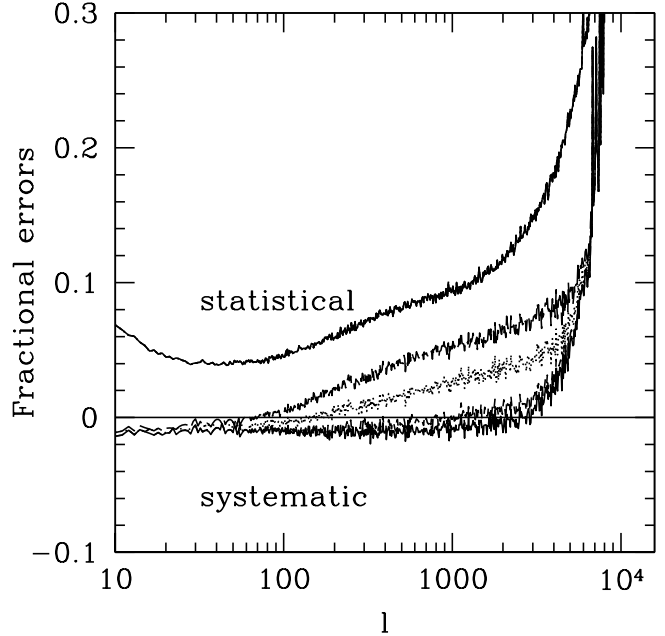


Figure 8. The dependence of lensing power spectrum determination on the amplitude of the quadratic bias ($\mathbf{b}^{(2)}$). We enlarge $\mathbf{b}^{(2)}$ by a factor of 2 (dash lines), 4 (dot lines) and 6 (long dash lines). The statistical error has negligible dependence on its amplitude. But the systematic error is sensitive to its amplitude and the resulting stochasticity.

redshift bin size or even use galaxies over the whole survey redshift range to perform the lensing reconstruction. In this case, the SKA galaxy radio continuum survey is also a good target. It is expected to detect ~ 5 billion radio galaxies over 30000 square degrees.¹⁰ Therefore we expect that we may at least realize the case of “S2”, possibly “S1”, and likely even better.

4.2. The impacts of galaxy biases

The galaxy intrinsic clustering is the major systematic contamination of weak lensing reconstruction through cosmic magnification. At the level of two-point statistics, it is completely fixed by the galaxy biases (linear, quadratic, etc.). The amplitude and the shape (flux dependence) of galaxy biases affect the lensing reconstruction differently. Therefore we investigate the two separately.

4.2.1. The impacts of galaxy bias amplitude

To isolate the impact of galaxy bias amplitude, we fix the shape of galaxy biases. We first arbitrarily enlarge the amplitude of $\mathbf{b}^{(1)}$ by a factor of 2, 4 and 10. Fig. 7 shows the corresponding statistical and systematic errors. Surprisingly, both errors show negligible dependences on the amplitude of $\mathbf{b}^{(1)}$. Interestingly, when we arbitrarily decreases $\mathbf{b}^{(1)}$ by a factor of 10, we find small but visible change in the systematic error. Even so, the statistical error remains unchanged. The insensitivity on the amplitude of $\mathbf{b}^{(1)}$ has a strong physical origin. We rely on the different flux dependences to separate the magnification bias from intrinsic clustering. Roughly

⁹ <https://pos.sissa.it/archive/conferences/215/017/AASKA14.017.pdf> ¹⁰ <https://pos.sissa.it/archive/conferences/215/018/AASKA14.018.pdf>

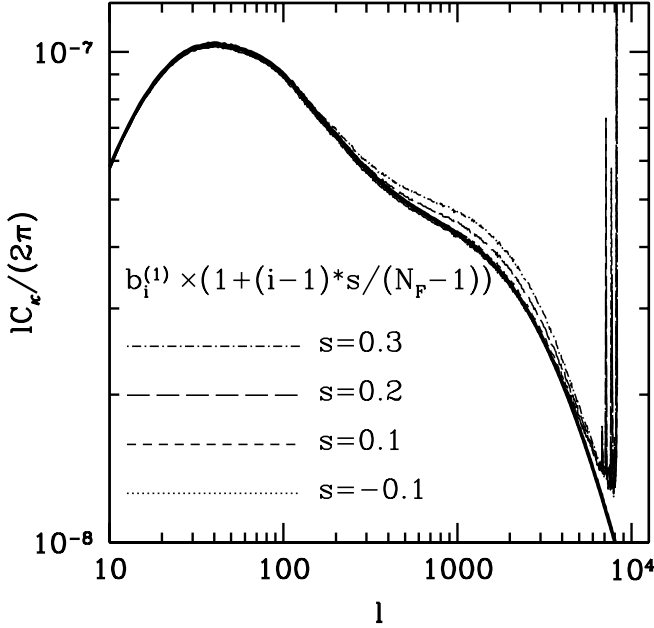


Figure 9. The dependence of lensing power spectrum determination on the shape of the deterministic bias $\mathbf{b}^{(1)}$. We change its shape from the faint end to the bright end by a factor of s .

speaking, we compare the difference in δ_g between bright and faint samples to extract/reconstruct the lensing signal. Therefore the lensing reconstruction is insensitive to the overall amplitude of $\mathbf{b}^{(1)}$, as long as it is the dominant part of galaxy biases.

We also enlarge $\mathbf{b}^{(2)}$ by a factor of 2, 4 and 6 to test our method (Fig. 8). Now the systematic error is sensitive to the amplitude of $\mathbf{b}^{(2)}$. The amplitude of $\mathbf{b}^{(2)}$ determines the stochasticity of intrinsic galaxy clustering. The stochasticity causes decorrelation between the galaxy overdensities of different flux bins. It then reduces the efficiency of extracting lensing signal by comparing between bright and faint galaxies. In contrast, we find surprisingly that the statistical error remains insensitive to the amplitude of $\mathbf{b}^{(2)}$.¹¹

Therefore we draw the conclusion that the lensing reconstruction accuracy is sensitive to the amplitude of $b^{(2)}$, but insensitive to that of $b^{(1)}$.

4.2.2. Impacts of galaxy bias shape

Since we rely on the difference in the flux dependences of the lensing signal and intrinsic clustering to reconstruct weak lensing, the lensing reconstruction accuracy is expected to depend on the shape of galaxy biases in flux space. We discuss two extreme cases to demonstrate this dependence. When $\mathbf{b} \parallel \mathbf{g}$, one can not separate the galaxy intrinsic clustering and the lensing magnification bias through their flux dependences. In contrast, when $\mathbf{b} \perp \mathbf{g}$, the lensing reconstruction would be most accurate. For the fiducial intrinsic clustering, $\mathbf{b}^{(1,2)}$ are nearly orthogonal to \mathbf{g} . However, this is not completely

¹¹ So far we do not have a solid explanation on this behavior. We suspect, but without a proof, that the prefactor η in Eq. 12 is invariant under the transformation $\mathbf{b}^{(1)} \rightarrow A\mathbf{b}^{(1)}$ (or $\mathbf{b}^{(2)} \rightarrow A\mathbf{b}^{(2)}$) where A is an arbitrary constant.

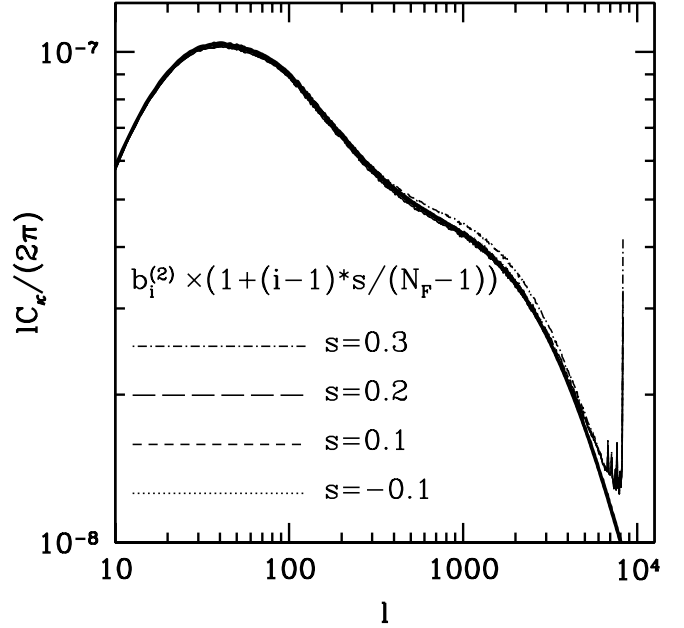


Figure 10. The dependence of lensing power spectrum determination on the shape of the quadratic bias $\mathbf{b}^{(2)}$. We change its shape from the faint end to the bright end by a factor of s .

coincident. Deep surveys probe not only bright galaxies with positive g_i , but also faint galaxies with negative g_i . Since $b_i^{(1)}$ is positive, $\mathbf{b}^{(1)} \cdot \mathbf{g}/(gb)$ is expected to be small.

To demonstrate the generality of our method, we arbitrarily modify $\mathbf{b}^{(1)}$ or $\mathbf{b}^{(2)}$ by the following recipe

$$b_i^{(1,2)} \rightarrow b_i^{(1,2)} \times \left[1 + s \times \frac{i-1}{N_F-1} \right]. \quad (15)$$

A positive s makes the shape of $\mathbf{b}^{(1)}$ less different to \mathbf{g} and therefore serves as more stringent test of our ABS method. We try different values of $s = -0.1, 0.1, 0.2, 0.3$, and the results are shown in Fig. 9. As expected, the reconstruction accuracy depends on the shape of biases. But even for change as large as 30% in shape, our ABS method still works to extract the lensing signal. Nevertheless, the systematic error increases to $\sim 10\%$ at $\ell = 2000$.

Fig. 6 shows the eigenmodes of the case $s = 0.3$ and the corresponding contribution factor c_μ , at multipole $\ell = 2000$. Since now the shape of $\mathbf{b}^{(1)}$ is significantly different to \mathbf{g} , it induces an extra (the third largest) eigenmode with significant $c_3 = 0.17$. When shot noise fluctuation is negligible ($\sigma_{\text{shot}} \ll \lambda_3$), the reconstruction of \tilde{C}_κ will be unbiased. But when shot noise fluctuation overwhelms ($\sigma_{\text{shot}} \gg \lambda_3$), this eigenmode will be completely missing. It will then lead to $c_\mu/(1-c_\mu) = 20\%$ overestimation of \tilde{C}_κ . The actual situation falls between the two extremes. The eigenmode has $\lambda_3 = 9.7 \times 10^{-12} \sim \sigma_{\text{shot}}/2$ (Fig. 2 at $\ell = 2000$, but noticing the $\ell^2/(2\pi)$ prefactor there). The resulting overestimation is 13% (Fig. 9).

Fig. 10 shows the impact of $\mathbf{b}^{(2)}$ shape on lensing reconstruction. The impact is significantly smaller than that of $\mathbf{b}^{(1)}$. This is again explained by the λ_μ - c_μ diagnostic. Fig. 6 shows the case of $s = 0.3$ (open

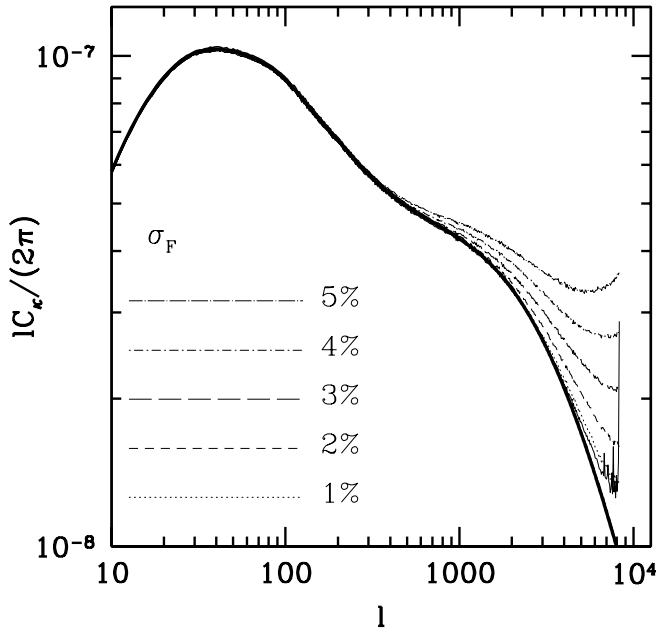


Figure 11. The dependence of lensing power spectrum determination on extra eigenmodes. By adding $\alpha_i^2 \sigma_F^2 / \bar{n}_g$ to the diagonal elements of C_{ij}^{obs} , we increase the rank of the matrix C_{ij}^{obs} to N_F , and therefore increase the difficulty of lensing reconstruction. Our ABS method still works for such extreme test. The observed systematic error is caused by observational limitation and will vanish in the limit of $\sigma_{\text{shot}} \rightarrow 0$.

square). Changing the shape of $\mathbf{b}^{(2)}$ by 30% also induces an eigenmode significant for lensing reconstruction, with $c_3 = 0.097$. This c_3 is a factor of 2 smaller than the case of $\mathbf{b}^{(1)}$. This explains the significantly smaller systematic error, comparing to that of $\mathbf{b}^{(1)}$.

Therefore we confirm our expectation that the shape of galaxy bias (flux dependence) is an important factor in weak lensing reconstruction. Realistic forecast of lensing reconstruction accuracy then relies on the reliability of the input fiducial galaxy bias model. But we want to emphasize two points. First, the lensing reconstruction itself does not rely on assumptions of the galaxy bias model, since we do not fit the data against any bias model. Second, the systematic error of lensing reconstruction is caused by survey limitation, instead of fundamental flaw in our method. This systematic error decreases and eventually vanishes if the galaxy number density is sufficiently high and the survey area is sufficiently large.

4.3. Impacts of extra components in the measured C_{ij}^{obs}

The measured matrix C_{ij}^{obs} can have extra principal components than discussed above. These extra components can be galaxy biases beyond the linear and quadratic bias (e.g. Hamaus et al. (2010)). They can also be uncorrected/miscorrected errors in the galaxy clustering measurement. Despite the difference in their physical origins, mathematically speaking they are similar. They will not only modify existing eigenmodes, but also generate extra eigenmodes. These extra eigenmodes increase the difficulty of lensing reconstruction therefore serve as more stringent tests of our ABS method.

Table 1

Cosmic magnification versus cosmic shear. The analogy of galaxy intrinsic clustering in cosmic magnification measurement is galaxy intrinsic alignment in cosmic shear measurement. Our ABS method can eliminate the galaxy intrinsic clustering, accurately and blindly.

Methods	cosmic shear	cosmic magnification
observable signal	$\epsilon^L = \epsilon_g + \gamma$ shear γ	$\delta_g^L = \delta_g + g\kappa$ convergence κ
systematic error	intrinsic alignment (correlated ϵ_g)	intrinsic clustering (correlated δ_g)
statistical error	random shape noise	shot noise

It is beyond the scope of this paper to fully explore these complexities. Instead, we will focus on a hypothetical case, but with some physical motivation. Observationally there are measurement errors in flux. As lensing magnification, such error in flux measurement also causes fluctuations in the galaxy number density, $\delta_g \rightarrow \delta_g + \alpha \delta_F$. Here, $\delta_F \equiv \delta F / F$ is the fractional flux measurement error. For random error ($\langle \delta_F \rangle = 0$), on the average it only affects the diagonal elements C_{ii}^{obs} . Its impact is inversely proportional to \bar{n} , similar to shot noise. In principle, we can predict its ensemble average and subtract it from the diagonal elements. However, *assuming that it is unnoticed and uncorrected in the measured C_{ii}^{obs}* , then

$$C_{ij}^{\text{obs}} \rightarrow C_{ij}^{\text{obs}} + \left(\alpha_i^2 \frac{\sigma_F^2}{\bar{n}_g} \right) \delta_{ij}. \quad (16)$$

Here $\sigma_F^2 \equiv \langle \delta_F^2 \rangle$. With its presence, the rank of the $N_F \times N_F$ matrix C_{ij}^{obs} will be N_F . Instead of extracting the lensing signal from contaminations of one or two components, now we need to deal with contaminations of N_F independent components. Strictly speaking, the mathematical proof of uniqueness of \tilde{C}_κ reconstruction and the associated analytical formula presented in this paper no longer hold. However, even in this extreme case, our ABS method still works well to some extent.

Fig. 11 shows the reconstruction accuracy when such error exists, for the case of $\sigma_F = 1\%$ - 5% . For $\sigma_F = 5\%$, \tilde{C}_κ can still be determined reasonably well. The systematic error is 1.4% at $\ell = 500$, 7% $\ell = 1000$, and 19% at $\ell = 2000$.¹² Such systematic error decreases with decreasing σ_F and becomes negligible for $\sigma_F \lesssim 1\%$. Therefore the ABS method may still work well under this extreme condition. Nevertheless, it demonstrates that in lensing reconstruction through cosmic magnification, flux calibration and its correction in the galaxy number overdensity are important. Finally we remind that the adopted model of extra systematic error in galaxy power spectra measurement (Eq. 16) is largely hypothetical and in reality such error may not exist. The major purpose is to demonstrate the impact of extra eigenmodes in the galaxy power spectra on the lensing reconstruction.

5. DISCUSSIONS AND CONCLUSIONS

¹² For $\sigma_F = 5\%$, there are two extra (the third and the fourth) eigenmodes with $c_\mu > 0.01$ at $\ell = 2000$ (Fig. 6, open circle). But the resulting overestimation is significantly larger than $(c_3 + c_4)/(1 - c_3 - c_4) \simeq 0.05$ that we expect from the $\lambda_{\mu-c_\mu}$ diagnostic. The reason is that now the contamination to the lensing magnification bias has N_F independent components and the analytical result of Eq. 7 is no longer exact/unbiased.

This paper outlines the ABS method to reconstruct weak lensing power spectrum by counting galaxies. It works on the measured cross galaxy power spectra between different flux bins. Based on the analytical solution that we found, the lensing power spectrum can be determined by a few straightforward linear algebra operations. It does not rely on assumptions of galaxy intrinsic clustering, making it robust against uncertainties in modelling galaxy clustering. The only limiting factor is the galaxy survey capability. To reliably determine the lensing signal, the galaxy survey must be sufficiently wide and sufficiently dense. Qualitatively speaking, statistical fluctuations in the galaxy power spectrum measurement (e.g. shot noise, but not cosmic variance) must be subdominant to the lensing signal. This is challenging for stage III projects. But stage IV projects such as SKA and LSST, with capability of measuring billion galaxies over half the sky, are promising to realize such lensing measurement at $z \sim 1$ and $\ell \lesssim 5 \times 10^3$. Such measurement will be highly complementary to cosmic shear measurement by the same surveys.

Table 1 compares cosmic magnification and cosmic shear. (1) Statistical error. Cosmic shear has the advantage of a factor of 3 smaller statistical error per galaxy. But cosmic magnification has more galaxies to use, since faint and small galaxies without useful cosmic shear measurement can still be useful for cosmic magnification. Which has smaller statistical error then depends on the survey specifications, galaxy luminosity function and the threshold of selecting galaxies (e.g. Zhang & Pen (2005)). (2) Systematic error. The analogy of galaxy intrinsic clustering in cosmic magnification is the galaxy intrinsic alignment in cosmic shear. There are intensive efforts to eliminate/alleviate the intrinsic alignment (Troxel & Ishak (2015) and references therein). One class of efforts is independent of intrinsic alignment modelling, such as nulling (Joachimi & Schneider 2008, 2009) and self-calibration (Zhang 2010a,b; Troxel & Ishak 2012c,b,a). In contrast, there are significantly less efforts in dealing with the intrinsic clustering. This paper presents our latest result, the ABS method, towards this direction (Zhang & Pen 2005, 2006; Yang & Zhang 2011; Yang et al. 2015). Similar to self-calibration of intrinsic alignment, the ABS method does not rely on external data, nor cosmological priors. It does not sacrifice cosmological information of weak lensing, since it utilizes no information of the lensing signal κ . It only uses the information encoded in the prefactor g , which by itself contains only astrophysical information of galaxy luminosity function.

Our ABS method is straightforward to implement in data analysis. What it does is to post-process the observed galaxy power spectra, whose measurement is a routine exercise. Next we will target at specific surveys to make more realistic forecasts of the lensing reconstruction accuracy by counting galaxies. We will combine with N-body simulations and halo occupation distribution/conditional luminosity function (e.g. Jing et al. (1998); Yang et al. (2003); Zheng et al. (2005), to generate more realistic C_{ij}^{obs} .

This work was supported by the National Science Foundation of China (11603019, 11433001, 11621303, 11653003, 11320101002, 11403071, 11475148), National Basic Research Program of China (2015CB85701), Key Laboratory for Particle Physics, Astrophysics and Cosmology, Ministry of Education, and Shanghai Key Laboratory for Particle Physics and Cosmology (SKLPPC), and Zhejiang province foundation for young researchers (LQ15A030001).

REFERENCES

- Ade, P. A. R., Akiba, Y., Anthony, A. E., et al. 2014a, *Physical Review Letters*, 112, 131302
— 2014b, *Physical Review Letters*, 113, 021301
Albrecht, A., Bernstein, G., Cahn, R., et al. 2006, *ArXiv Astrophysics e-prints*, astro-ph/0609591
Alsing, J., Kirk, D., Heavens, A., & Jaffe, A. H. 2015, *MNRAS*, 452, 1202
Bartelmann, M. 1995, *A&A*, 298, 661
Bartelmann, M., & Schneider, P. 2001, *Phys. Rep.*, 340, 291
Bauer, A. H., Gaztañaga, E., Martí, P., & Miquel, R. 2014, *MNRAS*, 440, 3701
Becker, M. R., Troxel, M. A., MacCrann, N., et al. 2016, *Phys. Rev. D*, 94, 022002
Bonoli, S., & Pen, U. L. 2009, *MNRAS*, 396, 1610
Chang, C., Vikram, V., Jain, B., et al. 2015, *Physical Review Letters*, 115, 051301
Chiu, I., Dietrich, J. P., Mohr, J., et al. 2016, *MNRAS*, 457, 3050
Cooray, A., Holz, D. E., & Huterer, D. 2006, *ApJ*, 637, L77
Das, S., Sherwin, B. D., Aguirre, P., et al. 2011, *Physical Review Letters*, 107, 021301
Dodelson, S., & Vallinotto, A. 2006, *Phys. Rev. D*, 74, 063515
Duncan, C. A. J., Heymans, C., Heavens, A. F., & Joachimi, B. 2016, *MNRAS*, 457, 764
Duncan, C. A. J., Joachimi, B., Heavens, A. F., Heymans, C., & Hildebrandt, H. 2014, *MNRAS*, 437, 2471
Ford, J., Hildebrandt, H., Van Waerbeke, L., et al. 2014, *MNRAS*, 439, 3755
Fu, L., Kilbinger, M., Erben, T., et al. 2014, *MNRAS*, 441, 2725
Garcia-Fernandez, M., Sánchez, E., Sevilla-Noarbe, I., et al. 2016, *ArXiv e-prints*, arXiv:1611.10326
González-Nuevo, J., Lapi, A., Negrello, M., et al. 2014, *MNRAS*, 442, 2680
Hamaus, N., Seljak, U., Desjacques, V., Smith, R. E., & Baldauf, T. 2010, *Phys. Rev. D*, 82, 043515
Hanson, D., Hoover, S., Crites, A., et al. 2013, *Physical Review Letters*, 111, 141301
Heavens, A., Alsing, J., & Jaffe, A. H. 2013, *MNRAS*, 433, L6
Heymans, C., Van Waerbeke, L., Miller, L., et al. 2012, *MNRAS*, 427, 146
Hildebrandt, H., van Waerbeke, L., & Erben, T. 2009, *A&A*, 507, 683
Hildebrandt, H., van Waerbeke, L., Scott, D., et al. 2013, *MNRAS*, 429, 3230
Hildebrandt, H., Choi, A., Heymans, C., et al. 2016, *MNRAS*, 463, 635
Hildebrandt, H., Viola, M., Heymans, C., et al. 2017, *MNRAS*, 465, 1454
Hirata, C. M., Ho, S., Padmanabhan, N., Seljak, U., & Bahcall, N. A. 2008, *Phys. Rev. D*, 78, 043520
Hoekstra, H., & Jain, B. 2008, *Annual Review of Nuclear and Particle Science*, 58, 99
Huff, E. M., Eifler, T., Hirata, C. M., et al. 2014, *MNRAS*, 440, 1322
Huff, E. M., & Graves, G. J. 2014, *ApJ*, 780, L16
Jarvis, M., Sheldon, E., Zuntz, J., et al. 2016, *MNRAS*, 460, 2245
Jing, Y. P., Mo, H. J., & Boerner, G. 1998, *ApJ*, 494, 1
Jing, Y. P., Zhang, P., Lin, W. P., Gao, L., & Springel, V. 2006, *ApJ*, 640, L119
Joachimi, B., & Schneider, P. 2008, *A&A*, 488, 829
— 2009, *A&A*, 507, 105
Kilbinger, M., et al. 2013, *Mon. Not. Roy. Astron. Soc.*, 430, 2200
Mandelbaum, R., Rowe, B., Armstrong, R., et al. 2015, *MNRAS*, 450, 2963

- Matsubara, T. 2008, *Phys. Rev. D*, 77, 063530
- Ménard, B., Scranton, R., Fukugita, M., & Richards, G. 2010, *MNRAS*, 405, 1025
- Morrison, C. B., Scranton, R., Ménard, B., et al. 2012, *MNRAS*, 426, 2489
- Munshi, D., Valageas, P., van Waerbeke, L., & Heavens, A. 2008, *Phys. Rep.*, 462, 67
- Nishizawa, A. J., Takada, M., & Nishimichi, T. 2013, *MNRAS*, 433, 209
- Okamoto, T., & Hu, W. 2003, *Phys. Rev. D*, 67, 083002
- Padmanabhan, N., & White, M. 2009, *Phys. Rev. D*, 80, 063508
- Planck Collaboration, Ade, P. A. R., Aghanim, N., et al. 2014, *A&A*, 571, A17
- 2016, *A&A*, 594, A15
- Refregier, A. 2003, *ARA&A*, 41, 645
- Rudd, D. H., Zentner, A. R., & Kravtsov, A. V. 2008, *ApJ*, 672, 19
- Schmidt, F., Leauthaud, A., Massey, R., et al. 2012, *ApJ*, 744, L22
- Scranton, R., Ménard, B., Richards, G. T., et al. 2005, *ApJ*, 633, 589
- Seljak, U. 1996, *ApJ*, 463, 1
- Seljak, U., & Zaldarriaga, M. 1999, *Physical Review Letters*, 82, 2636
- Smith, K. M., Zahn, O., & Doré, O. 2007, *Phys. Rev. D*, 76, 043510
- Smith, R. E., Peacock, J. A., Jenkins, A., et al. 2003, *MNRAS*, 341, 1311
- Troxel, M. A., & Ishak, M. 2012a, *MNRAS*, 427, 442
- 2012b, *MNRAS*, 423, 1663
- 2012c, *MNRAS*, 419, 1804
- 2015, *Phys. Rep.*, 558, 1
- Vallinotto, A., Dodelson, S., & Zhang, P. 2011, *Phys. Rev. D*, 84, 103004
- van Engelen, A., Keisler, R., Zahn, O., et al. 2012, *ApJ*, 756, 142
- van Engelen, A., Sherwin, B. D., Sehgal, N., et al. 2015, *ApJ*, 808, 7
- Wang, L., Cooray, A., Farrah, D., et al. 2011, *MNRAS*, 414, 596
- Weinberg, D. H., Mortonson, M. J., Eisenstein, D. J., et al. 2013, *Phys. Rep.*, 530, 87
- White, M. 2004, *Astroparticle Physics*, 22, 211
- Wyithe, J. S. B., Yan, H., Windhorst, R. A., & Mao, S. 2011, *Nature*, 469, 181
- Yang, X., Mo, H. J., & van den Bosch, F. C. 2003, *MNRAS*, 339, 1057
- Yang, X., & Zhang, P. 2011, *MNRAS*, 415, 3485
- Yang, X., Zhang, P., Zhang, J., & Yu, Y. 2015, *MNRAS*, 447, 345
- Zhan, H., & Knox, L. 2004, *ApJ*, 616, L75
- Zhang, P. 2010a, *MNRAS*, 406, L95
- 2010b, *ApJ*, 720, 1090
- 2015, *ApJ*, 806, 45
- Zhang, P., & Pen, U.-L. 2005, *Physical Review Letters*, 95, 241302
- 2006, *MNRAS*, 367, 169
- Zhang, P., Zhang, J., & Zhang, L. 2016, *ArXiv e-prints*, arXiv:1608.03707
- Zheng, Z., Berlind, A. A., Weinberg, D. H., et al. 2005, *ApJ*, 633, 791

APPENDIX

THE FIDUCIAL MODEL OF GALAXY BIASES

The two biases ($b^{(1,2)}$) are given in term of the derivations of the halo mass function (Matsubara 2008; Padmanabhan & White 2009; Nishizawa et al. 2013),

$$b^{(1)}(M_{\text{DM}}, z) = \frac{1}{\delta_c} \left[\nu^2 - 1 + \frac{2p}{1 + (q\nu^2)^p} \right] + 1, \quad (\text{A1})$$

$$b^{(2)}(M_{\text{DM}}, z) = \frac{1}{\delta_c^2} \left[q^2 \nu^4 - 3q\nu^2 + \frac{2p(2q\nu^2 + 2p - 1)}{1 + (q\nu^2)^p} \right] + \frac{8}{21}(b^{(1)} - 1).$$

Where $\nu = \delta_c(z)/\sigma(M_{\text{DM}})$. $\sigma(M_{\text{DM}})$ is the linearly evolved rms density fluctuation with a top-hat window function and $\delta_c(z) = 1.686/D(z)$. Here, p and q are parameters in the mass functions. The PS mass function is given with $p = 0$ and $q = 1$. HI galaxies are selected by their neutral hydrogen mass M_{HI} . To calculate the associated biases of these galaxies, we need to convert M_{HI} to M_{DM} . We simply choose $f_{\text{HI}} = M_{\text{HI}}/M_{\text{DM}} = 0.1$. We caution that the adopted bias model has several simplifications, and therefore may not well represent that in realistic survey. First, we have neglected the δ_m - δ_m^2 cross correlation, which vanishes at large scales. Second, in principle we should also include the cubic bias since it contributes comparably to the power spectrum as the quadratic bias. Third, f_{HI} should depend on the halo mass. In the main text we have extended the above bias model to much general cases, and shown that our ABS method of lensing reconstruction is insensitive to details of galaxy bias.